Sci. Bull. (2016) 61(14):1138–1144
DOI 10.1007/s11434-016-1118-7

www.scibull.com
www.springer.com/scp

Article

Engineering Sciences

Ab initio prediction of borophene as an extraordinary anode material exhibiting ultrafast directional sodium diffusion for sodium-based batteries

Le Shi · Tianshou Zhao · Ao Xu · Jianbo Xu

Received: 9 May 2016 / Revised: 1 June 2016 / Accepted: 2 June 2016 / Published online: 18 June 2016

Abstract Density functional theory calculations and ab initio molecular dynamics simulations are performed to study the feasibility of using borophene, a newly synthesized two-dimensional sheet of boron, as an anode material for sodium-ion and sodium–oxygen batteries. The theoretical capacity of borophene is found to be as high as 1,218 mAh g^{-1} ($Na_{0.5}B$). More importantly, it is demonstrated that the sodium diffusion energy barrier along the valley direction is as low as 0.0019 eV, which corresponds to a diffusivity of more than a thousand times higher than that of conventional anode materials such as $Na_2Ti_3O_7$ and Na_3Sb. Hence, the use of borophene will revolutionize the rate capability of sodium-based batteries. Moreover, it is predicted that, during the sodiation process, the average open-circuit voltage is 0.53 V, which can effectively suppress the formation of dendrites while maximizing the energy density. The metallic feature and structural integrity of borophene can be well preserved at different sodium concentrations, demonstrating good electronic conductivity and stable cyclability.

Keywords Borophene · Sodium anode · Directional diffusion · Ultrafast diffusivity

1 Introduction

Sodium-ion and sodium–oxygen batteries have recently drawn considerable attention as a promising alternative to lithium-based batteries due to the abundance and low price of sodium element [1–6]. However, sodium is a highly reactive metal with low melting temperature, and also shares the same dendrite problem with lithium, all of which pose sever safety concern [7, 8]. Finding a suitable anode material is one of the most urgent tasks before the commercialization of sodium-based batteries. As the size of sodium atom, 1.02 Å, is bigger than that of lithium, 0.76 Å, many of the anode materials that are good for lithium-based batteries are unsuitable for sodium-based batteries. For example, graphite, a widely used anode material in lithium-ion batteries, showed extremely low capacity when used as a sodium intercalation anode [1]. Many possible materials, such as hard carbon, $NiCo_2O_4$ and Sn, have been tested for sodium-based batteries, but these materials suffer from low intercalation utility, slow kinetics and sever volume expansion [9–11]. Thus, finding a proper anode material with a large reversible capacity, high sodium diffusion rate and good structural stability is critically important for the development of sodium-based batteries.

In recent years, two-dimensional (2D) materials draw great attention as a new class of potential candidates for the anode material of sodium-based batteries. The loose packing between the 2D layers can accommodate the volume expansion caused by the insertion of sodium atoms and maintain the structural integrity. Many 2D materials, such as defective/doped graphene [12, 13], transition metal dichalcogenides (TMD) [14, 15], transition metal carbides (MXenes) [16, 17] and phosphorene [18, 19], have been explored as potential candidates for the anode material of

Electronic supplementary material The online version of this article (doi:10.1007/s11434-016-1118-7) contains supplementary material, which is available to authorized users.

L. Shi · T. Zhao (✉) · A. Xu · J. Xu
Department of Mechanical and Aerospace Engineering, The Hong Kong University of Science and Technology, Hong Kong, China
e-mail: metzhao@ust.hk

sodium-based batteries using first-principle method, and some of the predicted good performance have already been proven in experiments [20, 21]. Recently, borophene, a 2D sheet of boron, has been successfully synthesized by Mannix et al. [22]. The atomic structure of borophene was resolved experimentally for the first time after many theoretical predictions [23–25]. The 2D metallic feature and low atomic weight of borophene make it an attractive potential choice for the anode of sodium-based batteries. In this work, we comprehensively investigated the feasibility of employing borophene as anode material for sodium-based batteries using density functional theory (DFT) method. The calculation results show that borophene can not only provide a superhigh capacity (1,218 mAh g^{-1}), but also exhibit a directional ultrahigh sodium diffusivity, which is estimated to be more than a thousand times higher than that of conventional anode materials such as $Na_2Ti_3O_7$ [26] and Na_3Sb [27] and one to seven magnitudes higher than other previously reported 2D materials [12–19]. The ultrahigh diffusivity will revolutionize the rate capability of sodium-based batteries. At different sodium concentrations, the metallic feature and structural integrity of borophene can be well preserved, which ensure good electronic conductivity and stable cyclability. The calculated average open-circuit voltage (OCV) is 0.53 V, which is an appropriate value for sodium-based batteries to maintain a high energy density while effectively suppressing the dendrite formation. All the calculation results show that borophene is a prospective material for the anode of both sodium-ion and sodium–oxygen batteries.

2 Computational details

All the calculations were performed using ABINIT software package [28–30], with Perdew–Burke–Ernzerhof (PBE) generalized gradient approximation (GGA) [31] and projector augmented-wave (PAW) method [32]. The cutting-off energy was set to be 20 Ha, and the k-point mesh was set to be <0.01 $Å^{-1}$. All the structures have been fully optimized with a force tolerance of 0.01 eV $Å^{-1}$. A 5 × 3 supercell was used to study the binding and diffusion of sodium with a 20 Å vacuum spacing along the z-direction.

The binding energy was calculated as [33]

$$E_b = E_{\text{borophene+Na}} - E_{\text{borophene}} - \mu_{\text{Na}}, \quad (1)$$

where $E_{\text{borophene+Na}}$ is the total energy of the borophene after bind with sodium, $E_{\text{borophene}}$ is the total energy of borophene and μ_{Na} is the chemical potential of metallic sodium.

According to the Arrhenius equation [33, 34], the diffusion coefficient (D) of sodium can be estimated by

$$D \sim e^{\frac{-E_a}{k_B T}}, \quad (2)$$

where E_a is the activation energy (diffusion barrier), k_B is the Boltzmann constant and T is the environment temperature.

Ab initio molecular dynamics (AIMD) was used to evaluate the structural stability of borophene and the diffusion of sodium atom. The simulations were performed on a 5 × 3 borophene supercell at 300 K using NVT ensemble. The time step was set to be 1 fs and both simulations last 3 ps.

3 Results and discussion

3.1 Structure of borophene

The top and side view of the optimized structure of borophene is shown in Fig. 1a, b. Different from the flat honeycomb structure of graphene [35], according to Mannix et al. [22], borophene belongs to the *pmmn* space group and shows a buckling structure. Here, we distinguish the boron atoms at different heights with "peak" and "valley", where "peak" denotes those atoms at higher positions in the z-axis considered, and "valley" denotes those atoms at lower positions. The optimized lattice parameters are $a = 1.62$ Å and $b = 2.87$ Å, which agree well with experiment and previous calculation results [22, 36, 37]. According to previous calculations [22, 36], the phonon spectrum of free-standing borophene shows a small imaginary frequency near the Γ point, indicating its instability against long-wavelength transversal waves, which can be fixed by defects and may explain the observed stripe formation in experiment. In this work, AIMD simulation was performed to check the thermal stability of borophene at 300 K using a 5 × 3 supercell. The snapshot during the

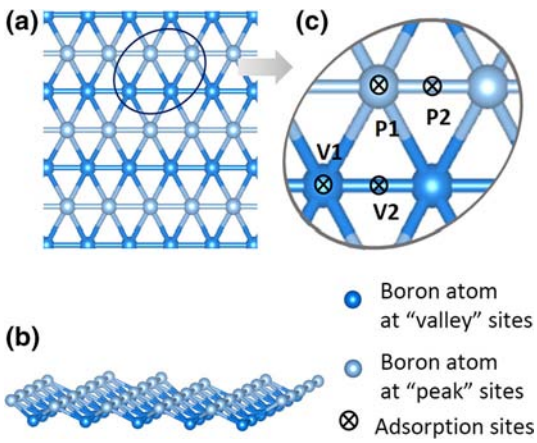

Fig. 1 (Color online) **a** Optimized borophene structure from top view and **b** side view, **c** the chosen adsorption sites on borophene

simulation process is shown in Fig. 2a. During the whole simulation process (3 ps), no broken bonds were observed. The movement of one boron atom was tracked as shown in Fig. S1 (online). It can be found that the chosen boron atom only vibrate around its initial position. The free energy of the supercell during the simulation is shown in Fig. 2b, and we can see the fluctuation is in a small range.

3.2 Adsorption of sodium onto borophene

To study the binding property of sodium on borophene, four different binding sites with high symmetry (V1, V2, P1, P2) have been investigated, as shown in Fig. 1c. The calculated binding energies for sodium at different sites are shown in Fig. 3a. All the binding energies have negative values lower than −1.2 eV, indicating a strong binding between sodium and borophene at all these four sites. The negative binding energies indicate that the sodium atoms tend to adsorb onto borophene uniformly instead of clustering and forming a separate phase of sodium metal, which can effectively suppress the formation of dendrites. The valley sites show stronger binding than the peak sites, while the energy differences between V1 and V2 or P1 and P2 are quite small. V1 site shows the largest adsorption energy of −1.50 eV, which is larger than that for lithium atom (−1.12 eV) [37]. The charge transfer between sodium and borophene when sodium adsorbed on V1 site is illustrated in Fig. 3b. The charge deficiency around sodium atom and charge sufficiency around nearby boron atoms indicate that the sodium atom loses its electrons to borophene and exists in the form of cation.

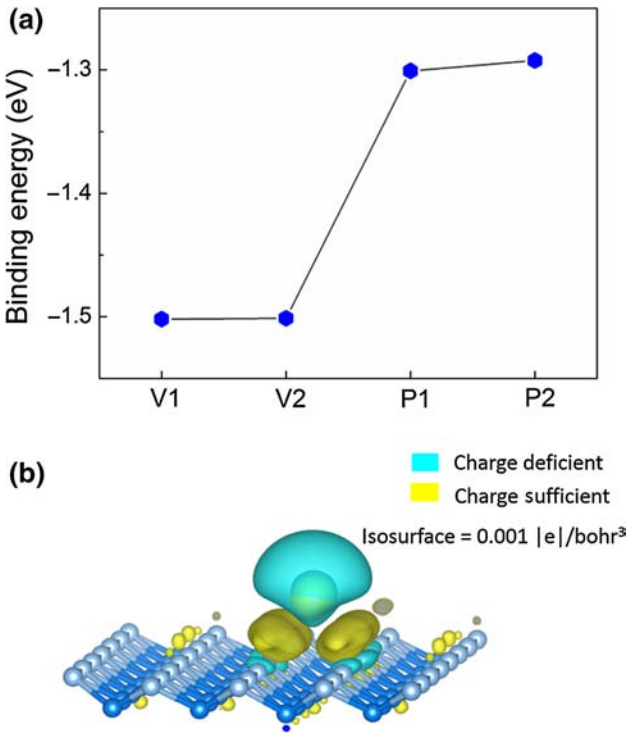

Fig. 3 (Color online) **a** Binding energies of sodium onto different adsorption sites of borophene, **b** the charge transfer for a single sodium atom binding onto borophene at V1 site

3.3 Migration of sodium on the surface of borophene

Three diffusion routes were chosen to study the diffusion of sodium on borophene. As illustrated in Fig. 4a, these

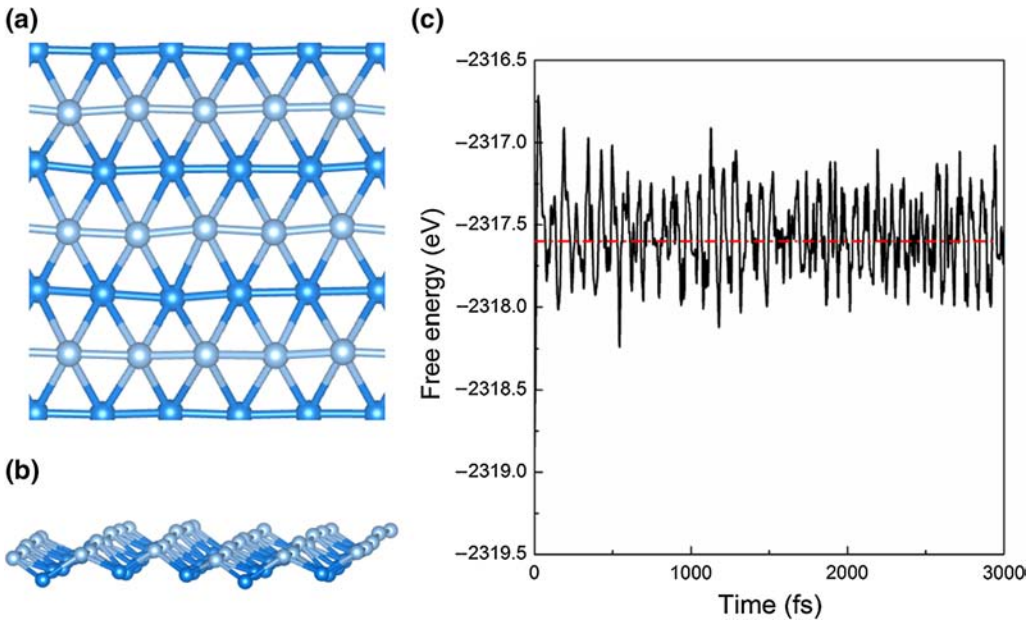

Fig. 2 (Color online) **a** Snapshot from AIMD simulation of geometrical structure of borophene from top view and **b** side view, **c** evolution of free energy for the borophene supercell during the simulation

three routes are labeled as "valley diffusion" (V1–V2–V1), "peak diffusion 1" (V1–P2–V1) and "peak diffusion 2" (V1–P1–V1). In "valley diffusion", sodium diffuses along the "valleys", while in "peak diffusion", sodium diffuses across the "peaks". Nudged elastic band (NEB) calculation was employed here to obtain the energy profiles. 9, 19 and 21 images were set for "valley diffusion", "peak diffusion 1" and "peak diffusion 2" according to the diffusion lengths. The obtained energy profiles are shown in Fig. 4b. Both "peak diffusion 1" and "peak diffusion 2" show a relative higher energy barrier of 0.24 and 0.25 eV, respectively, while "valley diffusion" exhibits an ultralow energy barrier of 0.0019 eV, which agree well with the above calculations on binding energies at different sites. This anisotropic diffusion property has also been predicted for lithium atom [37], which shows that the diffusion energy barrier along the valley direction is a bit higher (0.0026 eV) than sodium.

According to Eq. (2), the diffusivity of sodium along the valley direction at room temperature ($T = 300$ K) is about 10^4 times higher than those along the peak directions, which means the diffusion of sodium on borophene is strongly anisotropic and the diffusion along the peak directions are nearly impossible when compared with valley diffusion. The diffusion energy barrier for sodium in other investigated sodium anode materials such as $Na_2Ti_3O_7$ and Na_3Sb are 0.19 and 0.21 eV [27, 28], corresponding to diffusivities about more than 10^{-3} times lower that of the "valley diffusion" in borophene. When compared with other 2D materials, the energy barrier of "valley diffusion" is still ultralow and the diffusivity is one to seven magnitudes higher, as listed in Table S1 (online). This ultrahigh diffusivity along the valley direction indicates an excellent rate capability when using as anode material in sodium-based batteries.

AIMD simulation was also performed to evaluate the thermal stability of borophene after adsorbed with sodium atom. Similar with that of pure borophene, during the whole simulation time (3 ps), no broken bonds were observed and the fluctuation of the free energy of the system was in a small range as shown in Fig. S2a (online). More interestingly, when we track the movement of adsorbed sodium atom, it can be found that the sodium atom moved along the x-direction (valley direction) as shown in Fig. S2b (online). The simulation results indicate that sodium atoms could diffuse along the valley direction freely at 300 K. Similar behavior can not be observed along the y-direction (peak direction), which agree well with the anisotropic diffusion property calculated above. The high diffusion energy barrier along the peak direction could also effectively confine the sodium atoms in the valleys and prevent them from clustering.

3.4 Electrochemical properties of sodium adsorbed borophene

To study the adsorption behavior at higher sodium concentrations, six different Na/B ratios ($x = 0.0667$, 0.0833, 0.125, 0.167, 0.25 and 0.5) have been considered by employing 5×3, 4×3, 4×2 and 3×2 supercells. For each Na/B ratio, the sodium atoms were adsorbed onto both sides of borophene evenly, as shown in Fig. 5a–f. When the concentration of sodium increases, as shown in Fig. 5g, the absolute value of binding energy will decrease accordingly due to the repulsion of adjacent sodium atoms, while all the binding energies could keep negative lower than −0.5 eV. Thus, at high sodium concentrations, borophene can still exhibit a strong binding toward sodium. The charge transfer between the binding sodium and borophene is shown in Fig. S3 (online). In all the

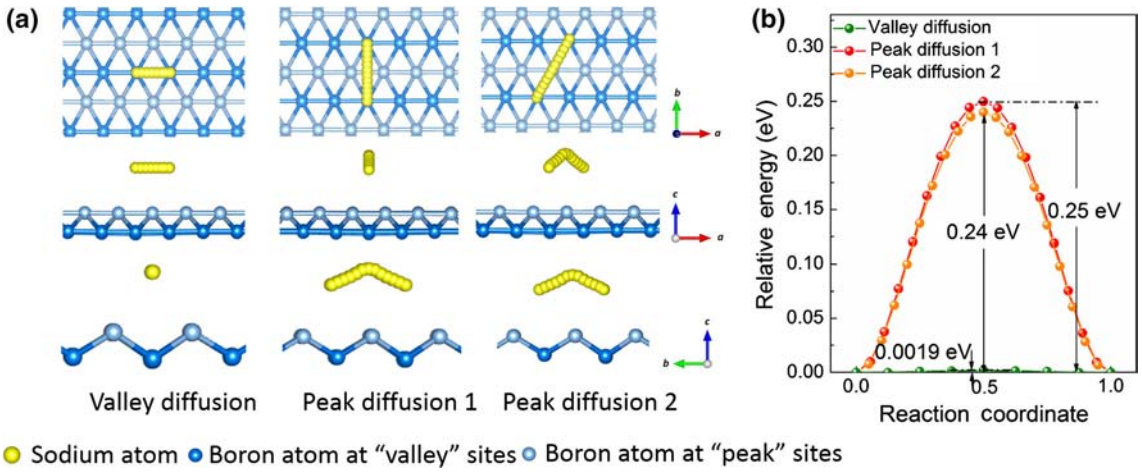

Fig. 4 (Color online) **a** Three considered diffusion routes for sodium on the surface of borophene. **b** The energy profiles for the considered diffusion routes

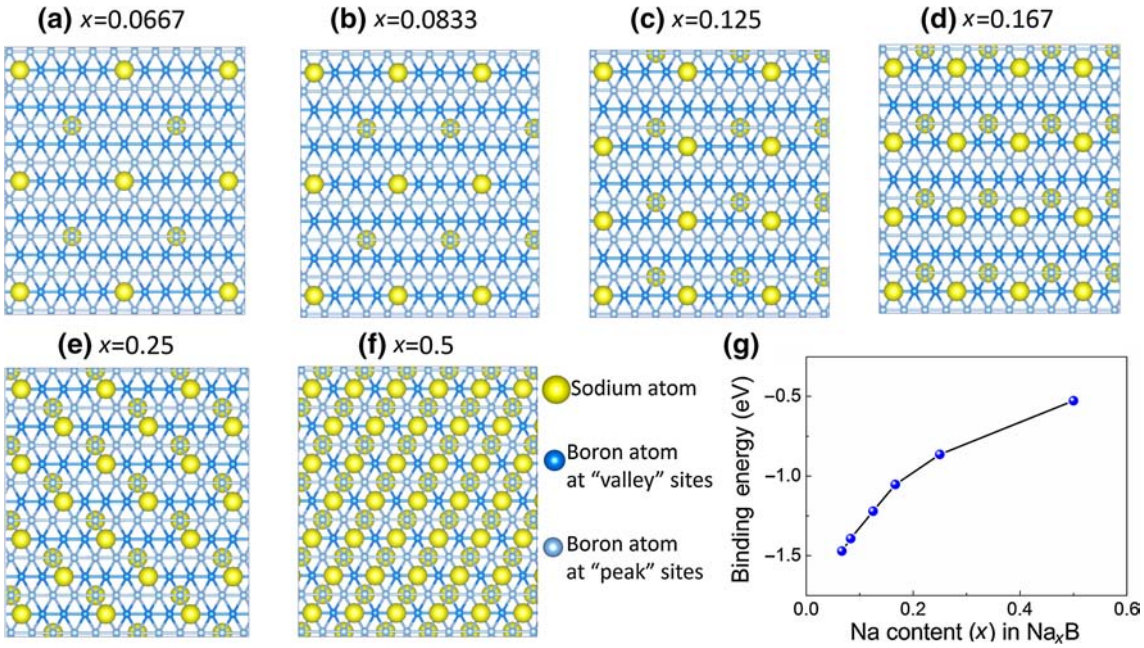

Fig. 5 (Color online) **a–f** The structures of Na_xB with different sodium concentrations. **g** The binding energy of sodium on borophene with different sodium concentrations

concentrations considered, the sodium atoms lose their electrons to borophene. When Na/B ratio reach 0.5, both sides of borophene will be fully covered by the sodium, and we regard this value to be the maximum capacity. The calculated corresponding theoretical capacity of $Na_{0.5}B$ is as high as 1,218 mAh g^{-1}, much higher than those reported in both experiments [9–11] and theoretical calculations (listed in Table S1 online). The theoretical capacity of borophene for sodium is a bit smaller than that for lithium [37] ($Li_{0.75}B$, 1,860 mAh g^{-1}), which is caused by the larger atomic radius. In practice, the borophene sheet may be not well separated. For stacked borophene, the Na on both sides of sheet is shared, and the maximum concentration will be reduced to half of the current estimation.

The open-circuit voltage (OCV) can be estimated using [38, 39]

$$\mathrm{OCV} \approx \frac{E_{\mathrm{Na}_{x1}\mathrm{B}} - E_{\mathrm{Na}_{x2}\mathrm{B}} + (x_2 - x_1)E_{\mathrm{Na}}}{(x_2 - x_1)e}, \quad (3)$$

where $E_{\mathrm{Na}_{x1}\mathrm{B}}$, $E_{\mathrm{Na}_{x2}\mathrm{B}}$ and E_{Na} are the energies of $Na_{x1}B$, $Na_{x2}B$ and metallic sodium, respectively. Figure 6a shows the OCV at various concentrations calculated using Eq. (3). Similar with the absolute value of binding energy, the OCV will decrease as the concentration of sodium

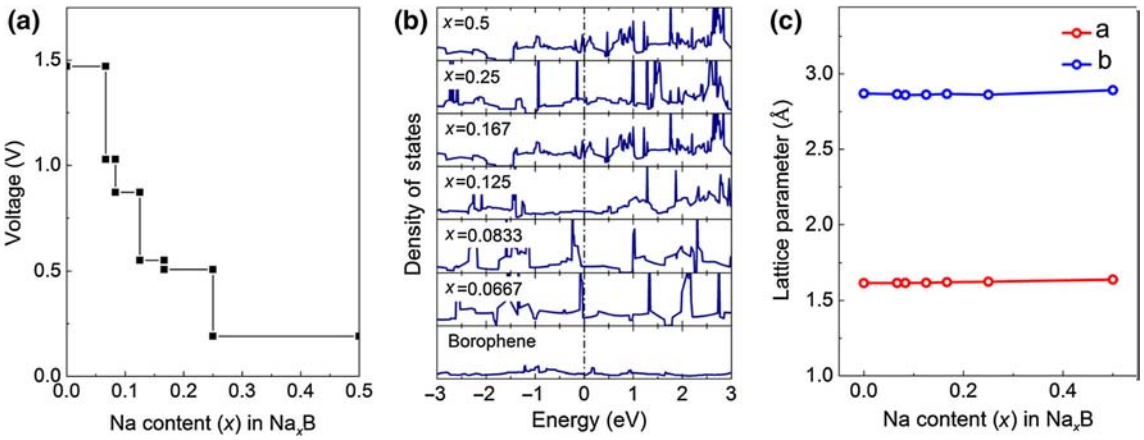

Fig. 6 (Color online) **a** The calculated voltage profile along the sodiation process. **b** The density of states (DOS) of borophene at different sodium concentration. **c** The lattice parameters of borophene at different sodium concentration

atoms increases. All the OCVs are lower than 1.5 V, and when the Na/B ratio exceeds 0.125, the OCV will become lower than 0.75 V. The calculated average OCV during the charge process is 0.53 V. This low theoretical OCV provides the feasibility of using this material as the anode in sodium-ion and sodium–oxygen batteries, which could maintain a high energy density while suppressing the dendrite formation.

3.5 Electronic properties and lattice deformation of borophene during the sodiation process

The density of states (DOS) of bare borophene before and after binding with sodium atoms at different concentrations are shown in Fig. 6b. All the considered systems are metallic, indicating a good electronic conductivity along with the discharge–charge process. Figure 6c showed the lattice parameters of borophene at different sodium concentrations. Even at a concentration as high as $Na_{0.5}B$, the volume expansion is <2 %. The fluctuations of lattice parameters along with the sodiation process are small, indicating a good structural stability when using as anode material for sodium-based batteries.

4 Conclusion

To summarize, we systematically investigated the feasibility of using the newly experimentally synthesized 2D metallic borophene as an anode material for sodium-based batteries. The calculation results show that borophene exhibits a superhigh specific capacity (1,218 mAh g^{-1}), good structural stability and more importantly, an extraordinary high diffusivity along valley direction, which is expected to revolutionize the rate capability of sodium-based batteries. The metallic feature of borophene can be well preserved along the whole sodiation process, ensuring good electronic conductivity. The calculated average OCV is 0.53 V, which is an appropriate value for sodium-ion and sodium–oxygen batteries to suppress the dendrite formation while maximizing the energy density. All the presented results suggest that borophene is a promising material for the anode of sodium-based batteries.

Acknowledgment This work was fully supported by a Grant from the Research Grants Council of the Hong Kong Special Administrative Region, China (16213414).

Conflict of interest The authors declare that they have no conflict of interest.

References

1. Slater MD, Kim D, Lee E et al (2013) Sodium-ion batteries. Adv Funct Mater 23:947–958
2. Pan H, Hu YS, Chen L (2013) Room-temperature stationary sodium-ion batteries for large-scale electric energy storage. Energy Environ Sci 6:2338–2360
3. Yabuuchi N, Kubota K, Dahbi M et al (2014) Research development on sodium-ion batteries. Chem Rev 114:11636–11682
4. Han MH, Gonzalo E, Singh G et al (2015) A comprehensive review of sodium layered oxides: powerful cathodes for Na-ion batteries. Energy Environ Sci 8:81–102
5. Xia C, Black R, Fernandes R et al (2015) The critical role of phase-transfer catalysis in aprotic sodium oxygen batteries. Nat Chem 7:496–501
6. Yadegari H, Banis MN, Xiao B et al (2015) Three-dimensional nanostructured air electrode for sodium–oxygen batteries: a mechanism study toward the cyclability of the cell. Chem Mater 27:3040–3047
7. Chevrier VL, Ceder G (2011) Challenges for Na-ion negative electrodes. J Electrochem Soc 158:A1011–A1014
8. Mortazavi M, Deng J, Shenoy VB et al (2013) Elastic softening of alloy negative electrodes for Na-ion batteries. J Power Sources 225:207–214
9. Ponrouch A, Goñi AR, Palacín MR (2013) High capacity hard carbon anodes for sodium ion batteries in additive free electrolyte. Electrochem Commun 27:85–88
10. Alcántara R, Jaraba M, Lavela P et al (2002) $NiCo_2O_4$ spinel: First report on a transition metal oxide for the negative electrode of sodium-ion batteries. Chem Mater 14:2847–2848
11. Liu Y, Zhang N, Jiao L et al (2015) Ultrasmall Sn nanoparticles embedded in carbon as high-performance anode for sodium-ion batteries. Adv Funct Mater 25:214–220
12. Datta D, Li J, Shenoy VB (2014) Defective graphene as a high-capacity anode material for Na- and Ca-ion batteries. ACS Appl Mater Interfaces 6:1788–1795
13. Ling C, Mizuno F (2014) Boron-doped graphene as a promising anode for Na-ion batteries. Phys Chem Chem Phys 16:10419–10424
14. Mortazavi M, Wang C, Deng J et al (2014) Ab initio characterization of layered MoS_2 as anode for sodium-ion batteries. J Power Sources 268:279–286
15. Yang E, Ji H, Jung Y (2015) Two-dimensional transition metal dichalcogenide monolayers as promising sodium ion battery anodes. J Phys Chem C 119:26374–26380
16. Yang E, Ji H, Kim J et al (2015) Exploring the possibilities of two-dimensional transition metal carbides as anode materials for sodium batteries. Phys Chem Chem Phys 17:5000–5005
17. Yu YX (2016) Prediction of mobility, enhanced storage capacity, and volume change during sodiation on interlayer-expanded functionalized Ti_3C_2 MXene anode materials for sodium-ion batteries. J Phys Chem C 120:5288–5296
18. Kulish VV, Malyi OI, Persson C et al (2015) Phosphorene as an anode material for Na-ion batteries: a first-principles study. Phys Chem Chem Phys 17:13921–13928
19. Hembram KP, Jung H, Yeo BC et al (2015) Unraveling the atomistic sodiation mechanism of black phosphorus for sodium ion batteries by first-principles calculations. J Phys Chem C 119:15041–15046
20. Xie X, Ao Z, Su D et al (2015) MoS_2/Graphene composite anodes with enhanced performance for sodium-ion batteries: the role of the two-dimensional heterointerface. Adv Funct Mater 25:1393–1403

21. Sun J, Lee HW, Pasta M et al (2015) A phosphorene–graphene hybrid material as a high-capacity anode for sodium-ion batteries. Nat Nanotechnol 10:980–985
22. Mannix AJ, Zhou XF, Kiraly B et al (2015) Synthesis of borophenes: anisotropic, two-dimensional boron polymorphs. Science 350:1513–1516
23. Lau KC, Pandey R (2007) Stability and electronic properties of atomistically-engineered 2D boron sheets. J Phys Chem C 111:2906–2912
24. Penev ES, Bhowmick S, Sadrzadeh A et al (2012) Polymorphism of two-dimensional boron. Nano Lett 12:2441–2445
25. Piazza ZA, Hu HS, Li WL et al (2014) Planar hexagonal B36 as a potential basis for extended single-atom layer boron sheets. Nat Commun 5:3113
26. Pan H, Lu X, Yu X et al (2013) Sodium storage and transport properties in layered $Na_2Ti_3O_7$ for room-temperature sodium-ion batteries. Adv Energy Mater 3:1186–1194
27. Baggetto L, Ganesh P, Sun CN et al (2013) Intrinsic thermodynamic and kinetic properties of Sb electrodes for Li-ion and Na-ion batteries: experiment and theory. J Mater Chem A 1:7985–7994
28. Gonze X, Beuken JM, Caracas R et al (2002) First-principles computation of material properties: the ABINIT software project. Comput Mater Sci 25:478–492
29. Gonze X, Amadon B, Anglade PM et al (2009) ABINIT: first-principles approach to material and nanosystem properties. Comput Phys Commun 180:2582–2615
30. Gonze X (2005) A brief introduction to the ABINIT software package. Zeitschrift für Kristallographie Cryst Mater 220:558–562
31. Perdew JP, Burke K, Ernzerhof M (1996) Generalized gradient approximation made simple. Phys Rev Lett 77:3865
32. Blöchl PE (1994) Projector augmented-wave method. Phys Rev B 50:17953
33. Jing Y, Zhou Z, Cabrera CR et al (2013) Metallic VS_2 monolayer: a promising 2D anode material for lithium ion batteries. J Phys Chem C 117:25409–25413
34. Li W, Yang Y, Zhang G et al (2015) Ultrafast and directional diffusion of lithium in phosphorene for high-performance lithium-ion battery. Nano Lett 15:1691–1697
35. Neto AC, Guinea F, Peres NM et al (2009) The electronic properties of graphene. Rev Mod Phys 81:109
36. Peng B, Zhang H, Shao H et al (2016) The electronic, optical, and thermodynamic properties of borophene from first-principles calculations. J Mater Chem C 4:3592–3598
37. Jiang HR, Lu Z, Wu MC et al (2016) Borophene: a promising anode material offering high specific capacity and high rate capability for lithium-ion batteries. Nano Energy 23:97–104
38. Ling C, Mizuno F (2012) Capture lithium in αMnO_2: insights from first principles. Chem Mater 24:3943–3951
39. Aydinol MK, Kohan AF, Ceder G et al (1997) Ab initio study of lithium intercalation in metal oxides and metal dichalcogenides. Phys Rev B 56:1354